

Partially Annealed Disorder and Collapse of Like-Charged Macroions

Yevgeni S. Mamasakhlisov · Ali Naji · Rudolf Podgornik

Received: 21 March 2008 / Accepted: 10 October 2008
© Springer Science+Business Media, LLC 2008

Abstract Charged systems with partially annealed charge disorder are investigated using field-theoretic and replica methods. Charge disorder is assumed to be confined to macroion surfaces surrounded by a cloud of mobile neutralizing counterions in an aqueous solvent. A general formalism is developed by assuming that the disorder is partially annealed (with purely annealed and purely quenched disorder included as special cases), *i.e.*, we assume in general that the disorder undergoes a slow dynamics relative to fast-relaxing counterions making it possible thus to study the stationary-state properties of the system using methods similar to those available in equilibrium statistical mechanics. By focusing on the specific case of two planar surfaces of equal mean surface charge and disorder variance, it is shown that partial annealing of the quenched disorder leads to renormalization of the mean surface charge density and thus a reduction of the inter-plate repulsion on the mean-field or weak-coupling level. In the strong-coupling limit, charge disorder induces a long-range attraction

Y.S. Mamasakhlisov
Dept. of Molecular Physics, Yerevan State University, 1 Al. Manougian str., Yerevan 375025, Armenia

A. Naji
Materials Research Laboratory, University of California, Santa Barbara, CA 93106, USA

A. Naji (✉)
Dept. of Chemistry and Biochemistry, University of California, Santa Barbara, CA 93106, USA
e-mail: anaji@chem.ucsb.edu

A. Naji · R. Podgornik
Kavli Institute for Theoretical Physics, University of California, Santa Barbara, CA 93106, USA

R. Podgornik
Dept. of Physics, Faculty of Mathematics and Physics, University of Ljubljana, 1000 Ljubljana, Slovenia

R. Podgornik
Dept. of Theoretical Physics, J. Stefan Institute, 1000 Ljubljana, Slovenia

R. Podgornik
Lab. of Physical and Structural Biology, National Institutes of Health, Bethesda, MD 20892, USA

51 resulting in a continuous disorder-driven collapse transition for the two surfaces as the disorder
52 variance exceeds a threshold value. Disorder annealing further enhances the attraction
53 and, in the limit of low screening, leads to a global attractive instability in the system.

54
55 **Keywords** Classical charged systems · Like-charge attraction · Charge disorder · Partial
56 annealing

57 58 59 **1 Introduction**

60
61 Interaction of charged macromolecules (macroions) is essential for soft and biological materials
62 in order to maintain their complex structure and distinct functioning. In many cases, charge
63 patterns along macromolecular surfaces are inhomogeneous and exhibit a highly disordered
64 spatial distribution. DNA microarrays [1, 2], surfactant-coated surfaces [3–6], random
65 polyelectrolytes and polyampholytes [7, 8] present examples of such disordered charge
66 distributions. The charge pattern can be either set and quenched in the process of assembly
67 of these surfaces, or can exhibit various degrees of annealing when interacting with other
68 macromolecules in aqueous solutions. Disorder annealing in charged systems may result
69 from different sources; *e.g.*, finite mobility and mixing of charged units (lipids and proteins)
70 in lipid membranes [9], conformational rearrangement of DNA chains in DNA microarrays
71 [1, 2] and charge regulation of contact surfaces bearing weak acidic groups in aqueous solutions
72 [10–12], to name a few, all lead to annealing effects. In reality, one may deal with a
73 more complex situation where the surface charge pattern displays an intermediate character
74 [3–6] and thus may neither be considered as purely quenched (*i.e.*, with fixed random spatial
75 distribution) nor as purely annealed (*i.e.*, thermally equilibrated with the bulk solution).

76 Charge disorder appears to produce electrostatic features that are remarkably different
77 from those found in non-disordered systems. Mounting experimental evidence shows
78 that like-charged phospholipid membranes and fluid vesicles, which primarily contain mobile
79 surface charges, may undergo aggregation and fusion in the presence of multivalent
80 cations [9]. A similar behavior is observed with negatively charged mica surfaces exposed
81 to a solution of positively charged surfactants [3–6]; here formation of a random mosaic of
82 surfactant patches on apposing surfaces (after the surfactant is adsorbed from the bathing
83 solution onto the surfaces) leads to a long-range attraction and thus a spontaneous jump to
84 a collapsed state. Although this behavior is akin to the transition to the primary minimum
85 within the standard DLVO theory of weakly charged systems [13, 14], the attractive forces at
86 work here exceed the universal van-der-Waals forces [15] incorporated in the DLVO theory
87 by a few orders of magnitude [3–6].

88 In fact, the emergence of an instability is not captured by the standard theories of charged
89 systems that incorporate static, non-disordered charge distributions for macromolecular surfaces.
90 These theories cover both mean-field [13, 14, 16] or weak-coupling limit (including the
91 Gaussian-fluctuations correction around the mean-field solution [17–19]) as well as the
92 strong-coupling (SC) limit [20–24], where the central theme is the absence or emergence of
93 electrostatic correlations induced by neutralizing counterions in the system that give rise to
94 attractive interactions between like-charged objects. Both uniform [13, 14, 16, 22] as well as
95 modulated [25, 26] charge distributions have been considered in this context. In the mean-
96 field regime, like-charged objects always repel. While the opposite limit of strong coupling
97 (realized, *e.g.*, with high valency counterions, highly charged macroions, low medium dielectric
98 constant or low temperature [20–22]) is dominated by correlation-induced attractive forces
99 that can bring two apposing like-charged surfaces to very small separation distances.

At small separations, however, a universal repulsion due to the confinement entropy of intervening counterions sets in and *stabilizes* the system in a closely packed bound state with a finite surface-surface separation [20–22]. This is true even for surfaces of opposite (unequal) uniform charge distribution [27]. Therefore, other mechanisms have to be at work that would lead to attractions strong enough to counteract such repulsive forces and lead to collapse or instability in a system of charged macroions. One such mechanism we propose is the disorder of the charge distribution along macromolecular surfaces that turns out to be as significant as the counterionic correlations and could provide a new paradigm in the theory of charged soft matter.

Previous studies of charge disorder on macromolecular surfaces have investigated both types of quenched [7, 8, 28–31] and annealed [7, 8, 30–36] disorder (including, specifically, the classical work on charge-regulating surfaces [10–12]). They mainly deal with situations where the system is in equilibrium and, on the question of electrostatic interaction [34–36], focus primarily on the weak-coupling regime, where disordered surfaces of equal mean charge always repel and no collapse or instability arises.¹ A systematic analysis of quenched disorder effects is presented in the previous works of two of the present authors [28, 29], where it was shown that not only can electrostatic interactions between like-charged objects turn from repulsive to attractive due to counterionic correlations, but also the disorder of the surface charge itself can give rise to an additive long-range attraction. This is most clearly demonstrated by attraction induced between disordered surfaces of *zero* mean charge but with a finite variance of the disordered charge distribution [29]. In the SC limit, the quenched disorder-induced attraction may be so strong that it can dominate the entropic repulsion at small separations and continuously shrink the SC surface-surface bound state [20–22] upon increasing the quenched disorder variance, predicting thus a *continuous collapse transition* between a stable and a collapsed phase beyond a threshold disorder variance [28]. Since the experimental situation may be more complex [3–6], and it might not allow for straightforward differentiation of the charge pattern into purely quenched and purely annealed cases, we next set ourselves to explore possible effects from partial annealing of the surface charge. If there is a fingerprint of the partially annealed surface charge disorder on the nature and magnitude of surface interactions, this would help in assessing whether the experimentally observed interactions can be interpreted in terms of disorder-induced interactions or not. This is the motivation with which we venture on this exploration.

In this paper, we present a general formalism for charged systems with partially annealed disorder by invoking field-theoretic and replica methods. We then focus on the case of two interacting *planar* charged surfaces as a model system and examine explicitly the effects of disorder on the inter-surface interaction in this system. Partially annealed disorder in general arises when a coupled motion of slow and fast variables (corresponding here to surface charges and counterions, respectively) is present in the system. It represents a non-equilibrium situation, whose investigation requires suitable methods. The previously studied cases of static, non-disordered surface charge distribution [20–22] as well as quenched [28] and annealed surface charge distribution follow as special cases from our formalism. In the SC limit, we find that the system of two like-charged planar surfaces with neutralizing counterions becomes *globally unstable* upon annealing the quenched surface charge

¹A notable exception in the course of previous studies of quenched disorder, which however will not be considered here, is the case where dielectric discontinuities at bounding surfaces (or the presence of salt in between the bounding surfaces) are taken into account [29]. In this case attraction emerges even in the weak-coupling regime. Another and similar situation in which weak-coupling instabilities may arise is when membrane undulations are allowed; see, e.g., [16, 37–39].

and collapses into contact regardless of other system parameters due to strong attractive forces from the annealing effects. Hence, the quenched phase behavior is not stable against small annealing perturbations and is dramatically changed. However, stability may be restored in this system by adding a finite amount of added salt that screens out the long-range Coulomb interactions. In this case, we recover the continuous collapse transition between a stabilized closely packed bound state of the two surfaces and a collapsed state where the surfaces are in contact. This is qualitatively similar to the purely quenched case [28]. However, the partially annealed bound state shows a significantly larger attraction and a smaller optimal surface separation as compared to the quenched case. In other words, allowing for rearrangements of the macroion charges leads to configurations of lower free energy. Since the present formalism is quite general, we shall also study the mean-field limit, where (in contrast to the quenched case where no disorder effects are found [28, 30, 31]) the disorder annealing appears to suppress the mean-field repulsion significantly by renormalizing the surface charge to smaller values. Hence, besides the previously established mechanisms of counterion-induced [22–24] and quenched disorder-induced [28, 29] correlations, we find that the annealing of macroion charges provides another mechanism enhancing the like-charge attraction.

The organization of the paper is as follows: We start with the general formalism that allows us to define and to deal with the partially annealed disorder in terms of an “effective partition function” that is obtained in the form of a functional integral over a fluctuating local electric potential field. The structure of this field theory is too complicated to allow for a general solution. We thus derive asymptotic solutions in the mean-field limit (corresponding to the Poisson-Boltzmann theory of the classical DLVO framework) as well as the strong-coupling limit *via* an application of the replica formalism. We finally evaluate and analyze the inter-surface interactions for the specific case of planar charged surfaces in both limits and compare them. We conclude by positioning our results in the growing framework of the weak–strong coupling formalism for charged macromolecular interactions.

2 General Formalism

Let us consider a system of *fixed* macroions with disordered charge distribution, $\rho(\mathbf{r})$, immersed in an aqueous medium of dielectric constant, ϵ , along with their point-like neutralizing counterions of valency q . In what follows, we shall develop our formalism for an arbitrary ensemble of fixed macroions but for explicit calculations, we shall delimit ourselves to a model system of two apposed charged planar surfaces with $\rho(\mathbf{r})$ representing the charge distribution along both planar surfaces (see Fig. 1). In the quenched limit, $\rho(\mathbf{r})$ is assumed to be static and only counterions are subject to thermal fluctuations. In the annealed limit, both counterions and macroion charges are subject to fluctuations of comparable time scales (*i.e.*, $\tau_{ci} \sim \tau_s$ respectively) and thus mutually equilibrate. The intermediate situation of partially annealed disorder by definition occurs when there is a macroscopic separation of time scales between the so-called fast and slow variables as frequently observed in glassy systems [43, 44].

In the present context, counterions comprise the fast variables as they are dispersed and freely fluctuate in the bulk. Macroion surface charges are assumed to constitute the slow variables with the time scale $\tau_s \gg \tau_{ci}$ due to their disordered nature (as, *e.g.*, they are confined typically within closely packed or quasi-two-dimensional disordered regions such as in lipid bilayers [9], surfactant-coated surfaces or surface hemimicelles [3–6, 45–47]).

Under these conditions, the mutual equilibration of fast and slow variables is hindered. Counterions rapidly attain their equilibrium at bulk temperature T and thus, because of the

Partially Annealed Disorder and Collapse of Like-Charged Macroions

201
202
203
204
205
206
207
208
209
210
211
212
213
214
215
216
217
218
219
220
221
222
223
224
225
226
227
228
229
230
231
232
233
234
235
236
237
238
239
240
241
242
243
244
245
246
247
248
249
250

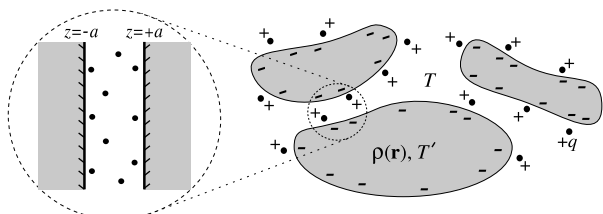


Fig. 1 Schematic view of a system of macroions with partially annealed disordered charge distribution $\rho(\mathbf{r})$ and q -valency counterions at bulk temperature T . Surface charges may exhibit a different effective temperature T' due to their disordered nature and slow dynamics relative to the fast-relaxing counterions. As a model system, we study two apposed planar macroion surfaces with disordered surface charge distributions (specified in the text) located at $z = \pm a$ at the separation distance $d = 2a$. We neglect the dielectric discontinuity at the boundaries or the presence of added salt in the system [29] (see also [40–42])

wide time-scale gap, their equilibrium free energy acts as a driving force pushing the slow dynamics of the surface charges to reach a non-equilibrium stationary state at long times. This scheme, known generally as the adiabatic elimination of fast variables [48–50], is investigated in a growing number of works, for instance, in the context of far-from-equilibrium stationary states and thermodynamics of two-temperature systems [51–54]. It has been applied in particular to study spin glasses with partially annealed disorder of the spin-spin coupling strength [43, 44, 55–64]. It has been shown in general that the stationary state of such systems may be described by a Boltzmann-type probability distribution featuring the temperature of fast degrees of freedom T as well as an effective temperature T' associated with the disorder. This peculiar two-temperature representation clearly reflects the intrinsically non-equilibrium nature of partial annealing. Obviously, the equilibrium free energy of fast variables (*i.e.*, counterions in our case) will show up explicitly in the aforementioned probability distribution (here we shall not consider the relaxational dynamics of the system and focus only on stationary-state properties).

In general, one may thus define an effective “partition function”, \mathcal{Z} , in analogy with the equilibrium partition function that greatly facilitates the analysis of the system far from equilibrium [43, 44, 52–64]. This procedure is discussed in Appendix A by adopting a simple dynamical model for a charged system with surface charge disorder and by identifying its stationary-state probability distribution. We thus find

$$\mathcal{Z} = \int \mathcal{D}\rho \exp(-\beta' \mathcal{W}[\rho]), \tag{1}$$

where $\beta' = \frac{1}{k_B T'}$ and the density functional $\mathcal{W}[\rho]$ can be cast into the form

$$\beta' \mathcal{W}[\rho] = \frac{1}{2} \int d\mathbf{r} g^{-1}(\mathbf{r}) [\rho(\mathbf{r}) - \rho_0(\mathbf{r})]^2 - n \ln \mathcal{Z}_{ci}[\rho], \tag{2}$$

where

$$n = \frac{T}{T'}. \tag{3}$$

Equation (2) includes statistics of both counterions and the disordered charges on macroion surfaces. The first term is the contribution of the disorder. It can be interpreted as a general effective disorder potential expanded to the second order around a typical value ρ_0 (Appendix A), which is always possible if one interprets $g(\mathbf{r})$ as playing the role of an effective

251 disorder “compressibility”. This expansion leads to the standard Gaussian disorder weight
 252 with the mean value $\rho_0(\mathbf{r})$ and variance $g(\mathbf{r})$ that can be handled most conveniently by
 253 replica techniques [43, 44]. Namely,

$$254 \mathcal{Z} = \int \mathcal{D}\rho \mathcal{P}[\rho] (\mathcal{Z}_{\text{ci}}[\rho])^n = \langle\langle (\mathcal{Z}_{\text{ci}}[\rho])^n \rangle\rangle, \quad (4)$$

255 where double-brackets denote the average $\langle\langle \dots \rangle\rangle = \int \mathcal{D}\rho \mathcal{P}[\rho] (\dots)$ with respect to the
 256 Gaussian probability distribution

$$257 \mathcal{P}[\rho] = C \exp\left(-\frac{1}{2} \int d\mathbf{r} g^{-1}(\mathbf{r}) [\rho(\mathbf{r}) - \rho_0(\mathbf{r})]^2\right) \quad (5)$$

258 with C being a normalization factor.

259 The second term in (2) is the equilibrium free energy of a system of counterions at a
 260 fixed realization of disordered macroion charge, $\rho = \rho(\mathbf{r})$. It follows by integrating over the
 261 counterionic degrees of freedom equilibrated at temperature T . In grand-canonical ensemble,
 262 the fixed- ρ partition function, $\mathcal{Z}_{\text{ci}}[\rho]$, can be cast into a form of a functional integral as
 263 [17–19, 22]

$$264 \mathcal{Z}_{\text{ci}}[\rho] = \int \frac{\mathcal{D}\phi}{\mathcal{Z}_v} e^{-\beta \mathcal{H}(\phi, \rho)}, \quad (6)$$

265 where $\phi(\mathbf{r})$ is the fluctuating electrostatic potential field, $\beta = \frac{1}{k_B T}$ and

$$266 \mathcal{H} = \int d\mathbf{r} \left[\frac{\varepsilon \varepsilon_0}{2} (\nabla \phi)^2 + i \rho \phi - \lambda k_B T \Omega(\mathbf{r}) e^{-i\beta q e_0 \phi} \right] \quad (7)$$

267 is the effective Hamiltonian of the system comprising Coulomb interaction $v(\mathbf{x}) =$
 268 $(4\pi \varepsilon \varepsilon_0 |\mathbf{x}|)^{-1}$ between all charged units (the first two terms) as well as the entropy of counterions
 269 (the last term). Here λ is the fugacity, $\mathcal{Z}_v = \sqrt{\det \beta v(\mathbf{r}, \mathbf{r}')}$, and $\Omega(\mathbf{r})$ is a geometry
 270 function that specifies the free volume available to counterions, *i.e.*, the space between the
 271 two apposed planar surfaces in the model system in Fig. 1.

272 The partition function (1) can be evaluated by using the replica trick [43, 44], *i.e.*, by
 273 taking n an integer number and then standardly extending the results to real axis (for any
 274 real value of $n = \beta'/\beta$) by analytical continuation. Thus by using (6) and averaging over
 275 $\rho(\mathbf{r})$, we arrive at the disorder-averaged expression

$$276 \mathcal{Z} = \int \left(\prod_{a=1}^n \frac{\mathcal{D}\phi_a}{\mathcal{Z}_v} \right) e^{-S[\{\phi_a\}]}, \quad (8)$$

277 where the n -replica effective Hamiltonian reads

$$278 S[\{\phi_a\}] = \frac{1}{2} \sum_{a,b} \int d\mathbf{r} d\mathbf{r}' \phi_a(\mathbf{r}) \mathcal{D}_{ab}(\mathbf{r}, \mathbf{r}') \phi_b(\mathbf{r}') \\ 279 + \sum_a \int d\mathbf{r} [i\beta \rho_0(\mathbf{r}) \phi_a(\mathbf{r}) - \lambda \Omega(\mathbf{r}) e^{-i\beta q e_0 \phi_a(\mathbf{r})}]. \quad (9)$$

280 The kernel $\mathcal{D}_{ab}(\mathbf{r}, \mathbf{r}')$ introduced above is defined as

$$281 \mathcal{D}_{ab}(\mathbf{r}, \mathbf{r}') = \beta v^{-1}(\mathbf{r}, \mathbf{r}') \delta_{ab} + \beta^2 g(\mathbf{r}) \delta(\mathbf{r} - \mathbf{r}'), \quad (10)$$

301 where $v^{-1}(\mathbf{r}, \mathbf{r}') = -\varepsilon\varepsilon_0\nabla^2\delta(\mathbf{r} - \mathbf{r}')$.

302 Equation (8) carries complete information about the mutual coupling between counte-
 303 rions and the surface charge disorder. The grand-canonical “free energy” of the partially
 304 annealed system is then obtained as

$$305 \mathcal{F} = -k_B T' \ln \mathcal{Z}. \tag{11}$$

306
 307
 308 The special cases of *purely quenched* and *purely annealed* disorder follow from (11) for
 309 $n \rightarrow 0$ and $n = 1$, respectively (see Appendix B).

310 Note that here the number of replicas, $n = T/T'$, has a direct physical meaning of temper-
 311 ature ratio [43, 44, 52–64]. A close examination of (9) indicates that the partially annealed
 312 disorder gives rise to quadratic surface terms of the form $g(\mathbf{r})\phi_a(\mathbf{r})\phi_b(\mathbf{r})$. It may thus lead
 313 to renormalization of the mean surface charge (Appendix C) as can be seen most clearly by
 314 looking at the mean-field equations which we shall derive next.

315 316 317 **3 Mean-Field Limit**

318
 319 The mean-field or Poisson-Boltzmann (PB) equation [13, 14, 16] (which becomes exact
 320 in the limit of small coupling parameters corresponding, for instance, to low counterion
 321 valency or low surface charge density [20–22]) follows from the saddle-point equation of
 322 the functional integral (8) as

$$323 \varepsilon\varepsilon_0\nabla^2\bar{\phi}_a = i\lambda q e_0 \Omega(\mathbf{r}) e^{-i\beta q e_0 \bar{\phi}_a(\mathbf{r})} + i\rho_0(\mathbf{r}) + \beta g(\mathbf{r}) \sum_b \bar{\phi}_b(\mathbf{r}). \tag{12}$$

324
 325
 326 We shall assume no preferences among different replicas on the saddle-point level, thus
 327 $\bar{\phi}_a(\mathbf{r}) = \bar{\phi}(\mathbf{r})$ for $a = 1, \dots, n$ (replica symmetry *ansatz*). In this way we arrive at the PB
 328 equation for the real-valued mean-field potential $\varphi_{\text{PB}}(\mathbf{r}) = i\bar{\phi}(\mathbf{r})$ as

$$329 \varepsilon\varepsilon_0\nabla^2\varphi_{\text{PB}}(\mathbf{r}) = -\lambda q e_0 \Omega(\mathbf{r}) e^{-\beta q e_0 \varphi_{\text{PB}}(\mathbf{r})} - \rho_{\text{eff}}(\mathbf{r}), \tag{13}$$

330
331
332 where

$$333 \rho_{\text{eff}}(\mathbf{r}) \equiv \rho_0(\mathbf{r}) - \beta' g(\mathbf{r}) \varphi_{\text{PB}}(\mathbf{r}) \tag{14}$$

334
 335 is the effective (renormalized) macroion charge distribution (Appendix C). It is therefore
 336 seen that in the quenched limit (n or $\beta' \rightarrow 0$), the disorder effects completely vanish on the
 337 mean-field level and the PB theory coincides *exactly* with that of a non-disordered system
 338 of bare charge distribution $\rho_0(\mathbf{r})$ [28]. This is however not true for the partially annealed
 339 disorder ($n > 0$).

340 To proceed with the PB theory, we shall consider the specific case of two parallel charged
 341 plates located (normal to z -axis) at $z = -a$ and $z = +a$ at the separation distance $d = 2a$
 342 (Fig. 1). We take the mean charge distribution and its variance as

$$343 \rho_0(\mathbf{r}) = -\sigma e_0 [\delta(z + a) + \delta(z - a)] \tag{15}$$

$$344 g(\mathbf{r}) = g e_0^2 [\delta(z + a) + \delta(z - a)], \tag{16}$$

345
 346
 347 where $g \geq 0$ and without loss of generality we assume that $\sigma \geq 0$ (and thus $q \geq 0$). Counte-
 348 rions are assumed to be confined in between the plates (*i.e.*, $\Omega(\mathbf{r}) = 1$ for $|z| < a$ and zero
 349
 350

elsewhere), where (13) admits the well-known solution [13, 14, 16]

$$\varphi_{PB}(z) = \frac{1}{\beta q e_0} \ln \cos^2(Kz) \tag{17}$$

with $K^2 = 2\pi \ell_B q^2 \lambda$ to be determined from the electroneutrality condition stipulating that the total charge on the two surfaces should be equal to the total charge of the counterions. This leads to the equation for K of the form

$$K\mu \tan(Ka) = 1 + \gamma \ln \cos^2(Ka) \equiv \frac{\sigma_{\text{eff}}}{\sigma}. \tag{18}$$

Here $\mu = 1/(2\pi q \ell_B \sigma)$ is the Gouy-Chapman length, $\ell_B = e_0^2/(4\pi \epsilon \epsilon_0 k_B T)$ the Bjerrum length, and

$$\sigma_{\text{eff}} = \sigma + \beta' g e_0 \varphi_{PB}(a) \tag{19}$$

the renormalized surface charge density (14). The latter expression clearly reflects the mixed boundary conditions encountered here, resembling the situation in the classical charge-regulation problems [10–12]. The dimensionless parameter

$$\gamma = \frac{ng}{q\sigma} \tag{20}$$

gives a measure of the *disorder annealing* and is obviously proportional to the ratio $n = T/T'$ of the counterions and surface disorder temperatures.

The PB pressure, P_{PB} , acting between the plates is obtained from the standard definition $\beta P_{PB} = n_{PB}(z_0) - \frac{1}{2} \beta \epsilon \epsilon_0 (d\varphi_{PB}/dz)^2|_{z_0}$ [13, 14, 16] for an arbitrary $|z_0| < a$ as

$$\frac{\beta P_{PB}}{2\pi \ell_B \sigma^2} = (K\mu)^2. \tag{21}$$

The counterion number density profile between the plates, $n_{PB}(z) = \lambda e^{-\beta q e_0 \varphi_{PB}(z)}$ [13, 14, 16], is obtained as

$$\frac{n_{PB}(z)}{2\pi \ell_B \sigma^2} = \left(\frac{K\mu}{\cos Kz} \right)^2. \tag{22}$$

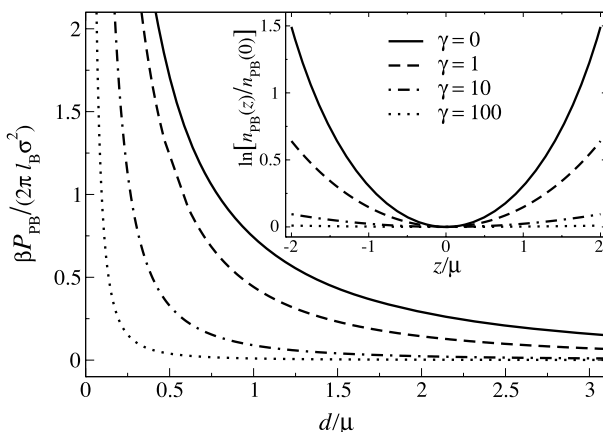
It follows from (18) that the mean-field renormalized surface charge density is always smaller than the bare value and tends to zero but never changes sign as γ increase ($0 \leq \sigma_{\text{eff}} \leq \sigma$). Therefore, the surfaces are effectively neutralized and the pressure as well as the counterion number density profile tend to zero as γ increases to infinity (see Fig. 2). This picture relies on the assumption that the number of surface charged units is not fixed and can respond to changes of the surface potential. Imposing the constraint that fixes this number obviously rules out surface charge renormalization and one observes no effects from the disorder annealing in agreement with [30, 31].

In the limit $\gamma \rightarrow 0$, we recover the non-disordered [22] or quenched [28] mean-field results with the following asymptotic behavior for the pressure,

$$\frac{\beta P_{PB}}{2\pi \ell_B \sigma^2} \simeq \begin{cases} 2\mu/d & d/\mu \ll 1, \\ \pi^2 \mu^2/d^2 & d/\mu \gg 1. \end{cases} \tag{23}$$

Partially Annealed Disorder and Collapse of Like-Charged Macroions

401 **Fig. 2** Rescaled PB pressure
 402 between two charged plates as a
 403 function of their separation d for
 404 $\gamma = 0, 1, 10$ and 10^2 . *Inset* shows
 405 the PB counterion density profile
 406 for $d/\mu = 4$. For $\gamma = 0$, we
 407 recover the non-disordered
 408 results with the pressure decaying
 409 as $\sim 1/d^2$ [22]. For $\gamma \gg 1$, the
 410 pressure decays as $\sim 1/(\gamma d^2)$



416 For large $\gamma \gg 1$, we find that $(Ka)^2 \simeq (\mu/a + \gamma)^{-1}$ and thus

418
$$\frac{\beta P_{PB}}{2\pi l_B \sigma^2} \simeq \begin{cases} 2\mu/d & \gamma d/\mu \ll 1, \\ 4\mu^2/(\gamma d^2) & \gamma d/\mu \gg 1. \end{cases} \quad (24)$$

421 The small separation expression above is nothing but the ideal-gas osmotic pressure of counterions that dominates over the energetic contributions. At large separations the pressure is found to decay asymptotically as $\sim 1/(\gamma d^2)$. The pressure remains always non-negative and the surface-surface interaction is thus always repulsive in the mean-field limit. Choosing the non-disordered system as the reference, however, the decrease in the interaction pressure upon increase of the surface disorder annealing can be interpreted as being due to an effective disorder-induced attraction whose asymptotic form could be described by

429
$$\Delta P_{PB} \sim \frac{1-\gamma}{\gamma} \frac{1}{d^2} \quad (25)$$

432 for large γ . This asymptotic form again attests to the fact that the way the disorder acts on the mean-field interaction between the two apposed surfaces is *via* a renormalization of the surface charge density.

437 **4 Strong-Coupling (SC) Limit**

438
 439 Next we shall investigate the asymptotic strong-coupling limit which is complementary to the mean-field limit and where counterion-induced correlations become dominant. We employ the standard strong-coupling scheme reviewed extensively in [20–22] in order to study the partial annealing effects in the SC limit. The so-called asymptotic SC theory is obtained from the leading order terms of a non-trivial virial expansion (in powers of the fugacity) of the partition function (8), *i.e.*

446
$$\mathcal{Z} = \mathcal{Z}_0 + \lambda \mathcal{Z}_1 + \mathcal{O}(\lambda^2). \quad (26)$$

448 It becomes exact in the limit of large coupling parameters corresponding, for instance, to high counterion valency or high surface charge density [20–22].

The zeroth-order (no counterion) term, \mathcal{Z}_0 , and the first-order (single counterion) term, \mathcal{Z}_1 , follow from (8) as

$$\mathcal{Z}_0 = \int \left(\prod_{a=1}^n \frac{\mathcal{D}\phi_a}{\mathcal{Z}_v} \right) e^{-S_0}, \tag{27}$$

$$\mathcal{Z}_1 = \sum_{b=1}^n \int d\mathbf{R}\Omega(\mathbf{R}) \int \left(\prod_{a=1}^n \frac{\mathcal{D}\phi_a}{\mathcal{Z}_v} \right) e^{-S_0 - i\beta q e_0 \phi_b(\mathbf{R})}, \tag{28}$$

where

$$S_0 = \frac{1}{2} \sum_{a,b} \int d\mathbf{r}d\mathbf{r}' \phi_a(\mathbf{r}) \mathcal{D}_{ab}(\mathbf{r}, \mathbf{r}') \phi_b(\mathbf{r}') + i\beta \sum_a \int d\mathbf{r} \rho_0(\mathbf{r}) \phi_a(\mathbf{r}). \tag{29}$$

We thus need to calculate both these terms for an arbitrary number of replicas, n . In doing so, we shall make use of some mathematical relations that we briefly discuss below.

4.1 Mathematical Preliminaries

First, it turns out that the most convenient way to carry out the calculations is to replace the long-range Coulomb interaction $v(\mathbf{x}) = 1/(4\pi\epsilon\epsilon_0|\mathbf{x}|)$ with the exponentially screened Yukawa interaction

$$v_s(\mathbf{x}) = \frac{e^{-\kappa|\mathbf{x}|}}{4\pi\epsilon\epsilon_0|\mathbf{x}|} \tag{30}$$

by introducing a finite screening length κ^{-1} . In the end, we shall take the limit $\kappa \rightarrow 0$. Note that not only is this procedure of technical convenience but it is also of physical relevance for the present problem. It corresponds to adding a background salt to the system, leading to the screened Coulomb interaction between charged units. It is to be noted however that the salt effects are taken into account in this way only on the linear Debye-Hückel level. (Further study of the role of added salt in the SC limit is presented elsewhere [42].) Generalization of (8)–(10) in the presence of Yukawa interaction is immediate as $v^{-1}(\mathbf{r}, \mathbf{r}')$ is simply replaced by

$$v_s^{-1}(\mathbf{r}, \mathbf{r}') = \epsilon\epsilon_0(-\nabla^2 + \kappa^2)\delta(\mathbf{r} - \mathbf{r}'). \tag{31}$$

Second, in calculating \mathcal{Z}_0 and \mathcal{Z}_1 one needs to evaluate the determinant and the inverse of the block-matrix $\mathcal{D}_{ab}(\mathbf{r}, \mathbf{r}')$. These calculations are straightforward and may be carried out most easily by employing properties of block-matrices and the operator algebra defined over the Hilbert space $\{|\mathbf{r}\rangle\}$. We shall use the compact notation by defining the operators $\langle \mathbf{r}|\hat{v}_s|\mathbf{r}'\rangle = v_s(\mathbf{r}, \mathbf{r}')$, $\langle \mathbf{r}|\hat{g}|\mathbf{r}'\rangle = g(\mathbf{r})\delta(\mathbf{r}, \mathbf{r}')$ (for the screened Coulomb interaction and disorder variance), and $\langle \mathbf{r}|\hat{\mathbf{D}}_{ab}|\mathbf{r}'\rangle = \mathcal{D}_{ab}(\mathbf{r}, \mathbf{r}')$ via (10), where the latter is defined as an element of the $n \times n$ operator matrix

$$\hat{\mathbf{D}} = \beta \mathbf{e} \otimes \hat{v}_s^{-1} + \beta^2 \mathbf{u} \otimes \hat{g} \tag{32}$$

with $\mathbf{e}_{ab} = \delta_{ab}$ and $\mathbf{u}_{ab} = 1$. Also, we shall use $\langle \mathbf{r}|\rho_0\rangle = \rho_0(\mathbf{r})$ and the well-known notation $\int_{\mathbf{r}, \mathbf{r}'} \rho_0(\mathbf{r}) v_s(\mathbf{r}, \mathbf{r}') \rho_0(\mathbf{r}') = \langle \rho_0|\hat{v}_s|\rho_0\rangle$, etc.

One can prove the following identities for $\hat{\mathbf{D}}$

$$\det \hat{\mathbf{D}} = (\det \beta \hat{v}_s^{-1})^n \det (\hat{\mathbf{I}} + n\beta \hat{g} \hat{v}_s), \tag{33}$$

$$\beta \sum_a \langle \mathbf{r} | (\hat{\mathbf{D}}^{-1})_{ab} | \mathbf{r}' \rangle = \langle \mathbf{r} | \hat{v}_s (\hat{\mathbf{1}} + n\beta \hat{g} \hat{v}_s)^{-1} | \mathbf{r}' \rangle, \tag{34}$$

$$\beta \langle \mathbf{r} | (\hat{\mathbf{D}}^{-1})_{aa} | \mathbf{r} \rangle = \langle \mathbf{r} | \hat{v}_s [\hat{\mathbf{1}} - \beta \hat{g} \hat{v}_s (\hat{\mathbf{1}} + n\beta \hat{g} \hat{v}_s)^{-1}] | \mathbf{r} \rangle, \tag{35}$$

which will be used in what follows. Note that the last two quantities do not depend on the replica indices a and b .

4.2 Virial Terms \mathcal{Z}_0 and \mathcal{Z}_1

Going back to the virial term \mathcal{Z}_0 , one can perform the Gaussian integral in (27) to obtain

$$\mathcal{Z}_0 = C_0 e^{-\frac{n}{2} \ln \det \beta \hat{v}_s - \frac{1}{2} \ln \det \hat{\mathbf{D}} - \frac{1}{2} \beta^2 \sum_{a,b} \langle \rho_0 | (\hat{\mathbf{D}}^{-1})_{ab} | \rho_0 \rangle}. \tag{36}$$

Using (33) and (34), \mathcal{Z}_0 is completely determined. This term represents the interaction free energy of macroion charges in the absence of counterions.

Next, the Gaussian integral in (28) can be evaluated as

$$\mathcal{Z}_1 = n \mathcal{Z}_0 \int d\mathbf{R} \Omega(\mathbf{R}) e^{-\beta u(\mathbf{R})}, \tag{37}$$

where $u(\mathbf{R})$ is nothing but the single-counterion interaction energy with the macroion charges and reads

$$u(\mathbf{R}) = \beta q e_0 \sum_a \langle \rho_0 | (\hat{\mathbf{D}}^{-1})_{ab} | \mathbf{R} \rangle + \beta \frac{(q e_0)^2}{2} \langle \mathbf{R} | (\hat{\mathbf{D}}^{-1})_{bb} | \mathbf{R} \rangle. \tag{38}$$

This is fully determined by virtue of (34) and (35). We have thus derived the general form of both virial terms in (26) as a function of n . We now proceed to the explicit evaluation of the two virial terms for the system of two apposed charged planar surfaces as defined by the mean charge distribution and disorder variance (15) and (16) (see Fig. 1).

4.3 Small- n Expansion

To proceed further we focus on the small- n limit of the above expressions. Our chief goal here is to examine the stability of the system upon small annealing perturbations of a quenched charge distribution. The annealing effects on this level are therefore expected to be additive in the free energy of the system.

By expanding (36) for small n we arrive at

$$\begin{aligned} \mathcal{Z}_0 \simeq C'_0 \exp \left(-\frac{n\beta}{2} \left[\text{Tr}(\hat{g} \hat{v}_s) + \langle \rho_0 | \hat{v}_s | \rho_0 \rangle \right] \right. \\ \left. + \frac{(n\beta)^2}{2} \left[\frac{1}{2} \text{Tr}(\{\hat{g} \hat{v}_s\}^2) + \langle \rho_0 | \hat{v}_s \hat{g} \hat{v}_s | \rho_0 \rangle \right] \right) \end{aligned} \tag{39}$$

to the lowest orders in n . But since we are interested in the inter-plate interaction, we shall need to determine only the separation-dependent terms.

It easily follows that the $\text{Tr}(\hat{g} \hat{v}_s)$ term in the above equation does not depend on the inter-surface distance $d = 2a$ and the $\text{Tr}(\{\hat{g} \hat{v}_s\}^2)$ term may be calculated straightforwardly (and up to an irrelevant additive term) as

$$\beta^2 \text{Tr}(\{\hat{g} \hat{v}_s\}^2) = -S(4\pi \ell_B^2 g^2) \text{Ei}(-2\kappa d), \tag{40}$$

where S is the total area of each surface and $\text{Ei}(x) = \int_{-\infty}^x dt e^t/t$ is the exponential-integral function. The remaining two terms in the expression for \mathcal{Z}_0 are obtained as

$$\beta \langle \rho_0 | \hat{v}_s | \rho_0 \rangle = 2S(\sigma^2 \ell_B) \left(\frac{2\pi}{\kappa} \right) (1 + e^{-\kappa d}), \tag{41}$$

$$\beta^2 \langle \rho_0 | \hat{v}_s \hat{g} \hat{v}_s | \rho_0 \rangle = 2S(g\sigma^2 \ell_B^2) \left(\frac{2\pi}{\kappa} \right)^2 (1 + e^{-\kappa d})^2. \tag{42}$$

The small- n expansion for \mathcal{Z}_1 leads to evaluation of $e^{-\beta u(\mathbf{R})} \simeq e^{-\beta u_0(\mathbf{R})} [1 + n\beta u_1(\mathbf{R})]$, where we have expanded $u(\mathbf{R}) = u_0(\mathbf{R}) - nu_1(\mathbf{R}) + \mathcal{O}(n^2)$ to the lowest order in n , and thus the following two terms

$$u_0(\mathbf{R}) = qe_0 \langle \rho_0 | \hat{v}_s | \mathbf{R} \rangle - \beta \frac{(qe_0)^2}{2} \langle \mathbf{R} | \hat{v}_s \hat{g} \hat{v}_s | \mathbf{R} \rangle, \tag{43}$$

$$u_1(\mathbf{R}) = \beta qe_0 \langle \rho_0 | \hat{v}_s \hat{g} \hat{v}_s | \mathbf{R} \rangle - \beta^2 \frac{(qe_0)^2}{2} \langle \mathbf{R} | \hat{v}_s \hat{g} \hat{v}_s \hat{g} \hat{v}_s | \mathbf{R} \rangle. \tag{44}$$

We have discarded a self-energy term $(qe_0)^2 \langle \mathbf{R} | \hat{v}_s | \mathbf{R} \rangle$ in (43) whose only effect is to rescale the fugacity, λ [28]. We can then use the explicit expressions

$$\beta e_0 \langle \rho_0 | \hat{v}_s | \mathbf{R} \rangle = -(\sigma \ell_B) \left(\frac{2\pi}{\kappa} \right) (e^{-\kappa|a-R_z|} + e^{-\kappa|a+R_z|}) \tag{45}$$

$$\beta^2 e_0 \langle \rho_0 | \hat{v}_s \hat{g} \hat{v}_s | \mathbf{R} \rangle = -(\sigma g \ell_B^2) \left(\frac{2\pi}{\kappa} \right)^2 (1 + e^{-\kappa d}) (e^{-\kappa|a-R_z|} + e^{-\kappa|a+R_z|}). \tag{46}$$

The two remaining expressions in (43) and (44) are obtained as

$$\beta^2 e_0^2 \langle \mathbf{R} | \hat{v}_s \hat{g} \hat{v}_s | \mathbf{R} \rangle = -(2\pi g \ell_B^2) [\text{Ei}(-2\kappa|a - R_z|) + \text{Ei}(-2\kappa|a + R_z|)], \tag{47}$$

$$\begin{aligned} \beta^3 e_0^2 \langle \mathbf{R} | \hat{v}_s \hat{g} \hat{v}_s \hat{g} \hat{v}_s | \mathbf{R} \rangle &= (2\pi g^2 \ell_B^3) \left(\frac{2\pi}{\kappa} \right) [(e^{-2\kappa|a-R_z|} + e^{-2\kappa|a+R_z|} + 2e^{-2\kappa d}) \\ &\quad + 2\kappa|a - R_z| \text{Ei}(-2\kappa|a - R_z|) + 2\kappa|a + R_z| \text{Ei}(-2\kappa|a + R_z|) \\ &\quad + 4\kappa d \text{Ei}(-2\kappa d)]. \end{aligned} \tag{48}$$

We shall need only the small κ results, which read (after discarding irrelevant constants)

$$\beta^2 e_0^2 \langle \mathbf{R} | \hat{v}_s \hat{g} \hat{v}_s | \mathbf{R} \rangle \simeq -(2\pi g \ell_B^2) \ln(a^2 - R_z^2), \tag{49}$$

$$\beta^3 e_0^2 \langle \mathbf{R} | \hat{v}_s \hat{g} \hat{v}_s \hat{g} \hat{v}_s | \mathbf{R} \rangle \simeq (2\pi g^2 \ell_B^3) \left(\frac{2\pi}{\kappa} \right) (e^{-2\kappa|a-R_z|} + e^{-2\kappa|a+R_z|} + 2e^{-2\kappa d}). \tag{50}$$

This completes the explicit evaluation of both virial terms. We now proceed to the evaluation of the interaction free energy, *i.e.*, the part of the free energy that explicitly depends on the separation between the two surfaces.

4.4 SC Free Energy

By using (36)–(38), one can evaluate the free energy of a partially annealed system from $\mathcal{F}^{\text{SC}} = -k_B T' \ln \mathcal{Z}$ (11), where $\mathcal{Z} = \mathcal{Z}_0 + \lambda \mathcal{Z}_1$ in the SC limit (26). The fugacity can be

fixed by the number of counterions N upon transforming to canonical ensemble *via*

$$nN = \lambda \frac{\partial \ln \mathcal{Z}}{\partial \lambda}, \tag{51}$$

whereby we obtain

$$\lambda = \frac{N}{\int d\mathbf{R}\Omega(\mathbf{R})e^{-\beta u(\mathbf{R})}}. \tag{52}$$

The canonical SC free energy is obtained *via* the Legendre transform, $\mathcal{F}_N^{\text{SC}} = \mathcal{F}^{\text{SC}} + Nk_B T \ln \lambda$, as

$$\frac{\beta \mathcal{F}_N^{\text{SC}}}{N} = -\frac{\ln \mathcal{Z}_0}{Nn} - \ln \int d\mathbf{R}\Omega(\mathbf{R})e^{-\beta u(\mathbf{R})} \tag{53}$$

supplemented by the electroneutrality condition, which for the two-plate system reads $Nq = 2\sigma_{\text{eff}}S$, and again stipulates that the total charge on the surfaces equals the charge of the interposed counterions. Note that here σ_{eff} is the effective surface charge density that has to be determined self-consistently within the SC theory. It turns out however that, in the SC limit, there is no charge renormalization due to partial annealing on the leading order in n , and thus $\sigma_{\text{eff}} = \sigma$ up to corrections of the order $\mathcal{O}(n^2)$ (see Appendix C). This behavior is in stark contrast with the one found on the mean-field level in Sect. 3.

The above expressions (51)–(53) together with (36)–(38) are applicable to any general system of fixed macroions with (Gaussian) disordered charge distribution and arbitrary degree of annealing n . For small annealing perturbations, we have

$$\frac{\beta \mathcal{F}_N^{\text{SC}}}{N} = -\frac{\ln \mathcal{Z}_0}{Nn} - \ln \int d\mathbf{R}\Omega(\mathbf{R})e^{-\beta u_0(\mathbf{R})} - n\beta \frac{\int d\mathbf{R}\Omega(\mathbf{R})\mu_1(\mathbf{R})e^{-\beta u_0(\mathbf{R})}}{\int d\mathbf{R}\Omega(\mathbf{R})e^{-\beta u_0(\mathbf{R})}} + \mathcal{O}(n^2), \tag{54}$$

where \mathcal{Z}_0 is given by (39).

In what follows, we shall focus again on the two-plate model system ((15) and (16)) and make use of the explicit expressions (40)–(50) in order to calculate the SC free energy of this system. We then take the limit of small inverse screening length, $\kappa \rightarrow 0$, as noted in Sect. 4.1. We thus find that the SC free energy of this system adopts a simple form as

$$\begin{aligned} \frac{\beta \mathcal{F}_N^{\text{SC}}}{N} &\simeq f_{\text{quenched}} + \frac{n}{\kappa} (8\pi^2 q \ell_B^2 g \sigma) d, \\ &= f_{\text{quenched}} + \left(\frac{2\gamma}{\kappa \mu} \right) \frac{d}{\mu}, \end{aligned} \tag{55}$$

where the first term on the right hand side, f_{quenched} , is nothing but the quenched ($n = 0$) rescaled free energy [28]

$$f_{\text{quenched}} = \frac{d}{2\mu} + (\chi - 1) \ln d, \tag{56}$$

and the second term in (55) represents the leading order correction from partial annealing of the disorder. Note that this term is linear in n as expected and scales with the inverse screening length κ^{-1} .

The quenched free energy (56) is expressed in terms of the dimensionless *disorder coupling parameter* $\chi = 2\pi q^2 \ell_B^2 g$, which gives a measure of the disorder-induced coupling *via*

651 the surface charge variance g . This is to be compared with the so-called *electrostatic cou-*
 652 *pling parameter* $\Xi = 2\pi q^3 \ell_B^2 \sigma$ defined originally for non-disordered systems [22], which
 653 measures the strength of counterion-induced correlations and, in the present context, de-
 654 pends on the mean charge density σ . The information about the disorder annealing enters
 655 only via $\gamma = ng/(q\sigma)$ as defined previously in (20). These dimensionless parameters may
 656 be used to determine the phase behavior of a partially annealed system, with the disorder
 657 effects being in general quantified by χ and γ .

658
 659 **4.5 Instability and Collapse Transition**
 660

661 The quenched free energy (56) comprises the standard non-disordered SC contributions, *i.e.*,
 662 the counterion-mediated attraction, $d/2\mu$, and the repulsion, $-\ln d$, due to the confinement
 663 entropy of counterions between the two surfaces [20–22]. But it also includes a long-range
 664 additive logarithmic term, that is $\chi \ln d$, stemming from the disorder variance which is at-
 665 tractive and renormalizes the repulsive entropic term. This peculiar form of the quenched
 666 disorder contribution leads to the previously predicted [28] *continuous collapse transition* at
 667 the threshold $\chi_c = 1$ between a stable bound state of the two surfaces and a collapsed state
 668 where the surfaces are in contact. In other words, the optimal surface-surface separation, d_* ,
 669 behaves as

670
 671
 672
$$\frac{d_*}{\mu} = \begin{cases} 2(1 - \chi) & \chi < 1, \\ 0 & \chi > 1. \end{cases} \quad (57)$$

 673

674 If on the other hand the disorder is partially annealed ($n > 0$), we see from (55) that the
 675 annealing generates a *linear* attractive term in the free energy, that is $\sim \gamma d/\kappa$. It adds up with
 676 and enhances the counterion-mediated attraction term (first term in (56)) exhibiting thus a
 677 complementary effect when compared to the quenched disorder contribution. The threshold
 678 of the collapse transition $\chi_c = 1$ remains intact up to small corrections of the order $\mathcal{O}(n)^2$
 679 and the partially annealed bound-state separation is obtained in the limit of small inverse
 680 screening length, κ , as

681
 682
$$\frac{d_*}{\mu} \simeq \begin{cases} \frac{2(1-\chi)}{1+4\gamma/\kappa\mu} & \chi < 1, \\ 0 & \chi > 1, \end{cases} \quad (58)$$

 683
 684

685 which is always smaller than the quenched value, reflecting again the enhanced surface-
 686 surface attraction in the case of partially annealed disorder.

687 Note that the optimal separation in the partially annealed case, (58), tends to zero,
 688 $d_* \rightarrow 0$, as the inverse screening length tends to zero $\kappa \rightarrow 0$. In other words, the system
 689 goes into a collapsed state regardless of other parameters exhibiting thus a *global attractive*
 690 *instability*. Hence, a quenched system of macroion charges and counterions is not stable
 691 with respect to annealing perturbations of the macroion charge distribution in the absence
 692 of screening effects. The stability may be achieved by adding a finite amount of added salt.
 693 Unfortunately, the effects of added salt have not yet been properly analyzed in the context
 694 of the SC theory (see [42] for a recent attempt) and it is presently difficult to go beyond the
 695 linear description adopted here for the salt screening effects.

696
 697
 698 ²Subleading terms of order $\mathcal{O}(n\kappa^0)$ can in general result in a small shift in the threshold value of χ . For
 699 instance, the $\text{Tr}(\{\hat{g}\hat{v}_s\}^2)$ term, (40), leads to a small reduction of the order $\mathcal{O}(n)$ as $\chi_c \simeq 1 - \gamma/4$.

5 Conclusion and Discussion

In this work we have analyzed the effects of partially annealed disorder in the distribution of macromolecular (macroion) charges on the interaction between two such macromolecular surfaces across a solution containing mobile neutralizing counterions. Recent experiments on decorated mica surfaces [3–6] covered with a random mosaic of positive and negative charged domains (stemming from the adsorption of cationic surfactants) clearly point to the existence of a strong attractive surface-surface interaction which, upon formation of such domains, collapses the system into a compact state with the surfaces being in contact. This behavior resembles the transition to a primary minimum within the DLVO theory [13, 14] although the attraction mechanism here is strictly non-DLVO [3–6] producing attractive electrostatic forces that are up to a few orders of magnitude larger than the universal van-der-Waals forces [15] as incorporated in the DLVO theory. Moreover, the emergence of an attractive instability or even a collapse transition is not predicted within the standard theories of electrostatic interactions between charged macromolecular surfaces (even between surfaces bearing opposite charges) pointing thus to the possible role of the surface charge disorder in the aforementioned collapse transition.

The AFM investigation of the surface texture of mica surfaces [3–6] can be performed only before the measurements of the inter-surface forces and can not be monitored while the two surfaces are brought closer together. One can thus not be sure whether the surface distribution of the charged domains along the surfaces changes on approach of the surfaces or not. This leads in general to three possible scenarios:

- the surface charge disorder is completely set by the method of preparation of the surfaces and does not change on approach of the surfaces (quenched disorder),
- the surface charge disorder responds to the changes in the separation of the surfaces just as fast as the mobile charged species (such as counterions) in the solution between the surfaces (annealed disorder),
- and lastly, the surface charge disorder does respond to the changes of the separation but with a much larger time-scale than the mobile charged species between the surfaces (partially annealed disorder).

As the experiment alluded to above gives only the inter-surface interaction as a function of the separation, one is thus lead to investigate the *fingerprnt* of these different scenarios on the behavior of the interaction. Since the effects of annealed [10–12, 30–36] and quenched [28–31] disorder have already been investigated theoretically, we follow up on these analyses by investigating the changes in the inter-surface forces wrought by the intermediate case, where it is assumed that there is a clear separation of relaxation time scales between the dynamics of the “external” surface charges (τ_s) and the mobile charges floating in the solvent between the surfaces (τ_{ci}), *i.e.*

$$\tau_s \gg \tau_{ci}. \quad (59)$$

Thus, the fluctuations in the intervening Coulomb fluid have time enough to relax to their local equilibrium state for each configuration of the surface charge disorder, which shows a much slower relaxation with changes in the surface separation. The origin of the different relaxation times for the surface and bulk dynamics could be manifold: the finite mobility and mixing of charged units on the macromolecular surfaces, such as appears in lipid bilayers with embedded charged proteins [9], conformational rearrangement of strongly charged DNA chains such as appears in DNA microarrays [1, 2] and charge regulation of contact surfaces bearing weak acidic groups in aqueous solutions [10–12], but should be in any case

751 very *system specific*. This separation of time scales is closely related to the so-called “adi-
 752 abatic elimination” of fast degrees of freedom [48–50], which has been used frequently in
 753 the literature for systems with widely different time scales [43, 44, 51–64] (see also Appen-
 754 dix A).

755 In this work we thus investigate the “interaction fingerprint” of the partially annealed
 756 disorder on two apposed planar surfaces upon their approach. The analysis presented above
 757 points to the fact that partial annealing of the surface charges invariably leads to additional
 758 attractive interactions between the surfaces and may even result in a global attractive insta-
 759 bility in the system. The nature of these attractions is quite different, however, if counterions
 760 are *strongly* or *weakly* coupled to charged surfaces in the sense of Netz [20–22]. The mag-
 761 nitude of this coupling essentially depends on the valency of counterions, q , the magnitude
 762 of the surface charge density, σe_0 , and the Bjerrum length $\ell_B = e_0^2 / (4\pi \epsilon \epsilon_0 k_B T)$ (incorpo-
 763 rating the medium temperature and dielectric constant), and is measured by the electrostatic
 764 coupling parameter

$$765 \quad \Xi = 2\pi q^3 \ell_B^2 \sigma. \quad (60)$$

767 For weakly coupled counterions, *i.e.* specifically in the mean-field limit ($\Xi \rightarrow 0$), the
 768 partially annealed disorder leads to smaller mean-field repulsions due to a renormalized
 769 (reduced) value of the surface charge density. The attraction in this case can thus be inferred
 770 only from a diminished repulsion with respect to the case of a non-disordered surface charge
 771 distribution. For strongly coupled counterions, *i.e.*, on the SC level ($\Xi \rightarrow \infty$), we derive
 772 explicitly an additional inter-surface attraction stemming from the partial annealing of the
 773 surface charge distribution. Note that the qualitative difference between the mean-field and
 774 the SC results goes back to the strong electrostatic correlation effects that are included in
 775 the SC theory but excluded on the mean-field level. The reason for this additional attraction
 776 (or reduction of the inter-surface repulsion in the mean-field limit) compared to the purely
 777 quenched case is that any rearrangement of the macroion charges, such as is assumed in
 778 partial annealing, inevitably leads to configurations of lower (free) energy which shows up
 779 as an effective attraction. This means that every disordered charged system will be unstable
 780 against annealing. In both the mean-field as well as the strong-coupling limit, the effect of
 781 partial annealing is quantified by a single partial annealing parameter

$$783 \quad \gamma = \frac{ng}{q\sigma}, \quad (61)$$

785 which depends on the temperature ratio $n = T/T'$. This is in addition to the disorder cou-
 786 pling parameter

$$788 \quad \chi = 2\pi q^2 \ell_B^2 g, \quad (62)$$

790 which measures the spread of the charge disorder distribution *via* the disorder variance g .

791 The parameter γ and the effective surface temperature T' may be estimated experimen-
 792 tally from the mobility (Γ_s) and the diffusion (D_s) coefficients of the surface charges and by
 793 applying Einstein’s relation $k_B T' = D_s / \Gamma_s$ (Sect. A.1). The temperature ratio quantifying
 794 the effects of partial annealing can thus be cast into an equivalent form

$$796 \quad n = (k_B T) \frac{\Gamma_s}{D_s}. \quad (63)$$

798 How does one differentiate the effects of quenched and partially annealed disorder? Com-
 799 paring the results derived in the quenched case [28, 29] with those obtained in this work, one

801 realizes that in the former case the effects of the disorder are limited to the strong-coupling
 802 limit, while in the partially annealed case they persist also in the mean-field limit. This is
 803 because in the mean-field limit the surface charge density is renormalized in the presence
 804 of partially annealed disorder. This effect is always absent in the quenched disorder case
 805 (Appendix C).

806 Moreover, we find that in the SC regime and in the limit of low screening $\kappa \rightarrow 0$, a
 807 charged system that may be stable in the presence of quenched charge disorder could become
 808 globally unstable and collapse upon partial annealing of the disorder. One should also note
 809 that for small non-zero screening and in the stable phase ($\chi < 1$), the system adopts a much
 810 smaller surface-surface distance in the partially annealed case than in the quenched case as
 811 the ratio between the optimal distances in these two cases is given by $(1 + 4\gamma/\kappa\mu)^{-1}$.

812 Another indicative feature of partially annealed disorder is the curious property that the
 813 surfaces interact electrostatically even if the mean surface charge density, σ , goes to zero,
 814 that is when the surfaces become *net* electroneutral! It may be seen most clearly from the
 815 $\text{Tr}(\{\hat{g}\hat{v}_s\}^2)$ term in (40), which in the limit $\kappa \rightarrow 0$ leads to a logarithmic attractive contri-
 816 bution in the free energy as $\simeq n\pi g^2 \ell_B^2 S \ln d$ stemming only from the variance, g , of the
 817 surface charge disorder (note however that when $\sigma > 0$ this is a subleading term compared
 818 to the additive $1/\kappa$ term considered in (55)) (see also footnote 2). This effect disappears in
 819 the quenched limit ($n \rightarrow 0$) unless either the dielectric discontinuities at bounding surfaces
 820 or the presence of salt in between the bounding surfaces are taken into account [29]. It is
 821 thus safe to say that the effects of partially annealed disorder are in general stronger and
 822 ubiquitous and may be qualitative in both mean-field and strong-coupling limits.

823 Nevertheless, though the above-mentioned interaction fingerprints would help in assess-
 824 ing the importance of disorder or even its presence in the charge distribution on macromole-
 825 cular surfaces, the interactions by themselves would not be enough to make this conclusion
 826 with a reasonable degree of certainty. Unfortunately, more detailed experiments where one
 827 would concurrently measure interactions as well as surface charge distributions would still
 828 be essential.

829 Our analysis of the effects of macromolecular charge disorder on their interactions sup-
 830 plements the recently acquired new wisdom of bio-colloidal interactions [20–24], as op-
 831 posed to its classical formulation [13, 14], in quite an illuminating way. Whereas on the
 832 DLVO or mean-field level [13, 14, 16] one can formulate the salient features of macro-
 833 molecular Coulomb interactions with the folk wisdom that opposites attract and likes repel,
 834 the strong-coupling paradigm [20–24] suggests that likes attract too if the system is highly
 835 charged. To this we would add, in view of our previous work [28, 29] and the work described
 836 above, that if the surface charge distribution is disordered, the system may become unstable
 837 and collapse due to attractive disorder-induced forces and that even neutral macromolecu-
 838 lar surfaces can interact *via* electrostatic interactions. This is especially true if the disorder
 839 distribution is partially annealed as we set to prove in this work.

840 **Acknowledgements** R.P. would like to acknowledge the support of Agency for Research and Development
 841 of Slovenia under grants P1-0055(C), Z1-7171 and L2-7080. This study was supported by the Intramural
 842 Research Program of the NIH, National Institute of Child Health and Human Development. This research
 843 was supported in part by the National Science Foundation under Grant No. PHY05-51164.

844 Appendix A: Dynamics of Disorder

845 A.1 Adiabatic Elimination of Fast Variables

846 The effective partition function for a partially annealed system may be obtained *via* an adi-
 847 abatic elimination of fast variables discussed widely in the literature [48–50]. Here we shall
 848
 849
 850

briefly discuss the extension of this method for a charged system with a slow disordered component. As described in the text we shall focus on a non-equilibrium system of mobile fast-relaxing counterions (located at positions $\xi_i(t)$ for $i = 1, \dots, N$, in a solvent of fixed temperature T) and a disordered ensemble of macroion surface charges (located at positions \mathbf{x}_i with $i = 1, \dots, N_s$ and bearing charges $q_s e_0$) which undergo a much slower dynamics. We shall be interested only in the stationary-state properties of the system. We adopt the Langevin equation for the dynamics of counterions and surface charges as

$$\dot{\xi}_i = -\Gamma_{ci} \frac{\partial H}{\partial \xi_i} + \theta_{ci}, \tag{64}$$

$$\dot{\mathbf{x}}_i = -\Gamma_s \frac{\partial H}{\partial \mathbf{x}_i} + \theta_s, \tag{65}$$

respectively, where the Hamiltonian H is written in terms of Coulomb pair interactions

$$H = \frac{1}{2} \sum_{i,j} v(\mathbf{x}_i, \mathbf{x}_j) + \sum_{i,j} v(\mathbf{x}_i, \xi_j) + \frac{1}{2} \sum_{i,j} v(\xi_i, \xi_j), \tag{66}$$

and θ_{ci} and θ_s are white noise terms with zero average and the two-point correlation function $\theta_{ci}(t) \cdot \theta_{ci}(t') = 6D_{ci} \delta(t - t')$ and $\theta_s(t) \cdot \theta_s(t') = 6D_s \delta(t - t')$. We impose Einstein's relations between the diffusion constants and the mobilities of the particle species, *i.e.*, $D_{ci} = k_B T \Gamma_{ci}$ and $D_s = k_B T' \Gamma_s$ that guarantee a stationary state may be achieved at long times. (We have neglected hydrodynamic interactions in (64) and (65) for simplicity as they do not affect the stationary-state results.)

The central assumption for the time scales of the counterions ($1/\Gamma_{ci}$) and the surface charges ($1/\Gamma_s$) translates into

$$\Gamma_s / \Gamma_{ci} \ll 1. \tag{67}$$

Our goal is to eliminate the fast (counterionic) variables that change at short time scales and obtain an *effective* dynamical equation for the slow (surface charge) variables assuming that the effective temperature of the latter, T' , may in general be different from that of the former, T [43, 44, 51–64]. This may be done readily given the condition (67) above and by developing a perturbative expansion (much in the spirit of the Born-Oppenheimer approximation) [48–50] in terms of the small parameter Γ_s / Γ_{ci} . The zeroth-order results are quite intuitive: one ends up with a Langevin equation for \mathbf{x}_i similar to (65) where the microscopic Hamiltonian H is replaced with an effective one, which is obtained by “pre-averaging” over the counterionic degrees of freedom; namely,

$$\dot{\mathbf{x}}_i = -\Gamma_s \frac{\partial H_{\text{eff}}}{\partial \mathbf{x}_i} + \theta_s, \tag{68}$$

where $H_{\text{eff}} = -k_B T \ln Z_{ci}$ and $Z_{ci} = \frac{1}{N!} \int \prod_i d\xi_i \exp(-\beta H)$. This effective Hamiltonian is of course nothing but the equilibrium free energy of counterions in the presence of a *fixed* realization of surface charges; its derivative acts as a driving force pushing the surface charge dynamics to reach a stationary state at long times with the Boltzmann-type probability weight $\exp(-\beta' H_{\text{eff}})$ as dictated by (68). Hence, the system—although far from equilibrium as a whole—may still be described in terms of an “effective” partition function, Z , once a stationary state is achieved, *i.e.*

$$Z = \frac{1}{N_s!} \int \left[\prod_i d\mathbf{x}_i \right] e^{-\beta' H_{\text{eff}}} = \frac{1}{N_s!} \int \left[\prod_i d\mathbf{x}_i \right] (Z_{ci})^n, \tag{69}$$

where $n = \beta'/\beta$.

A.2 Dynamical Density Functional Theory

It is possible to derive the n -replica partition function (8) directly from the expression (69) and by using a Legendre transformation to grand-canonical ensemble described by the partition functions $\mathcal{Z} = \sum_{N_s} \lambda_s^{N_s} Z$ and $\mathcal{Z}_{ci} = \sum_N \lambda^N Z_{ci}$, where λ_s and λ denote the fugacities of the surface charges and counterions, respectively. We shall however take a detour over the so-called dynamical density functional theory that first transforms the effective Langevin equation (68) into a dynamical equation for the surface charge density field $\rho(\mathbf{r}, t)$. This may be done straightforwardly following the approach proposed for classical fluids in [65–67]. One thus obtains

$$\frac{\partial}{\partial t} \rho(\mathbf{r}, t) = -\nabla \cdot \mathbf{J}_\rho(\mathbf{r}, t) + \eta(\mathbf{r}, t), \tag{70}$$

assuming a conserved density field [68, 69], where the current density reads

$$\mathbf{J}_\rho(\mathbf{r}, t) = -D_s \nabla \rho(\mathbf{r}, t) - (q_s e_0 \Gamma_s) \rho(\mathbf{r}, t) \nabla \langle \psi(\mathbf{r}, t) \rangle_T. \tag{71}$$

The first term on the right hand side represents the current due to the diffusion of surface charges and the second term represents the contribution from the mean effective electrostatic force acting on them; here $\langle \psi(\mathbf{r}, t) \rangle_T = -\delta \ln \mathcal{Z}_{ci}[\rho] / \beta \delta \rho(\mathbf{r})$ is the electrostatic potential at the *macroion surface* averaged over the counterionic degrees of freedom. The last term is a Gaussian white noise with $\langle \eta(\mathbf{r}, t) \rangle = 0$ and $\langle \eta(\mathbf{r}, t) \eta(\mathbf{r}', t') \rangle = 2\nabla \cdot \nabla' [D_s q_s e_0 \rho(\mathbf{r}, t) \delta(\mathbf{r} - \mathbf{r}') \delta(t - t')]$. Combining (70) and (71), one arrives at

$$\frac{\partial}{\partial t} \rho(\mathbf{r}, t) = \nabla \cdot (D_s \nabla \rho + (q_s e_0 \Gamma_s) \rho \nabla \langle \psi \rangle_T) + \eta(\mathbf{r}, t) \tag{72}$$

$$= \nabla \cdot \left[(q_s e_0 \Gamma_s) \rho(\mathbf{r}, t) \nabla \frac{\delta \mathcal{W}[\rho]}{\delta \rho(\mathbf{r}, t)} \right] + \eta(\mathbf{r}, t), \tag{73}$$

where the effective “potential”, $\mathcal{W}[\rho]$, follows as

$$\mathcal{W}[\rho] = \frac{1}{q_s e_0 \beta'} \int d\mathbf{r} \left[\rho \ln \left(\frac{\rho}{\rho_0} \right) - \rho \right] - \frac{1}{\beta} \ln \mathcal{Z}_{ci}[\rho] \tag{74}$$

with ρ_0 being a constant. Using a standard mapping of (73) to an equivalent Fokker-Planck equation, one can easily show that the stationary-state fluctuations of $\rho(\mathbf{r}, t)$ follow a Boltzmann-type weight $\exp(-\beta' \mathcal{W})$ and hence, the effective “partition function”

$$\mathcal{Z} = \int \mathcal{D}\rho e^{-\frac{1}{q_s e_0} \int d\mathbf{r} [\rho \ln(\rho/\rho_0) - \rho]} (\mathcal{Z}_{ci}[\rho(\mathbf{r})])^n. \tag{75}$$

In order to proceed with an analytical investigation, we assume that the surface density fluctuations around ρ_0 are small and expand the entropic term (first term in (74)) up to the second order, which gives $\rho \ln(\rho/\rho_0) - \rho \simeq (\rho - \rho_0)^2 / 2\rho_0$. One can generalize this result by assuming that different realizations of the surface charge disorder follow a Gaussian probability distribution as

$$\mathcal{P}[\rho] = C \exp \left(-\frac{1}{2} \int d\mathbf{r} g^{-1}(\mathbf{r}) [\rho(\mathbf{r}) - \rho_0(\mathbf{r})]^2 \right), \tag{76}$$

951 where C is a normalization factor and $g(\mathbf{r})$ is the disorder variance. The quadratic *ansatz*
 952 is completely general since it corresponds to an expansion in small deviations from $\rho_0(\mathbf{r})$
 953 where $g(\mathbf{r})$ can be interpreted as a disorder “compressibility”. One thus recovers (2) and (4)
 954 in the text.

955
 956 **A.3 Non-Conserved Disorder Dynamics**

957
 958 The dynamical model discussed above is based on a conserved model for the dynamics of
 959 the disorder, where the current density follows from the gradient of an effective chemical
 960 potential, *i.e.*, $\mathbf{J}_\rho = -(q_s e_0 \tilde{\Gamma}_s) \rho \nabla \mu_{\text{eff}}[\rho]$ with

961
 962
$$\mu_{\text{eff}}[\rho] \equiv \frac{\delta \mathcal{W}[\rho]}{\delta \rho} = \frac{1}{q_s e_0 \beta'} \ln \left(\frac{\rho}{\rho_0} \right) + \langle \psi(\mathbf{r}, t) \rangle_T \quad (77)$$

963
 964 as seen from (73). Alternatively, one could construct other dynamical models that include
 965 a non-conserved density field for the surface charge disorder and still give rise to the same
 966 effective partition function in the stationary-state limit [68, 69]. One may thus propose a
 967 phenomenological equation of the form

968
 969
$$\frac{\partial}{\partial t} \rho(\mathbf{r}, t) = -\tilde{\Gamma}_s (\mu_{\text{eff}}[\rho] - \mu_0) + \eta(\mathbf{r}, t), \quad (78)$$

970
 971 where $\tilde{\Gamma}_s$ is an effective mobility, μ_0 is a constant (which can be set to zero) and η is a
 972 Gaussian white noise with $\langle \eta(\mathbf{r}, t) \rangle = 0$ and $\langle \eta(\mathbf{r}, t) \eta(\mathbf{r}', t') \rangle = 2\tilde{D}_s \delta(\mathbf{r} - \mathbf{r}') \delta(t - t')$. Assuming
 973 $\tilde{D}_s = k_B T' \tilde{\Gamma}_s$ one can show that the partition function (75) is reproduced as the stationary-
 974 state solution. This model may be more appropriate to study dynamics of disorder in macro-
 975 molecules with ionizable surface groups.

976
 977
 978
 979 **Appendix B: Partially Annealed Free Energy**

980
 981 The “free energy” of a partially annealed disordered system follows from (4) as

982
 983
$$\mathcal{F} = -k_B T' \ln \mathcal{Z} = -k_B T' \ln \langle \langle \mathcal{Z}_{\text{ci}}^n \rangle \rangle. \quad (79)$$

984
 985 Obviously, the purely annealed disorder limit with true thermal equilibrium, $T = T'$, is
 986 recovered when $n = 1$,

987
 988
$$\mathcal{F}_{\text{annealed}} = -k_B T \ln \langle \langle \mathcal{Z}_{\text{ci}} \rangle \rangle, \quad (80)$$

989 while the purely quenched disorder limit follows by taking the limit $n \rightarrow 0$ (or $\beta' \rightarrow 0$).
 990 One can use $\langle \langle \mathcal{Z}_{\text{ci}}^n \rangle \rangle = e^{-\beta' \mathcal{F}}$ and expand both sides of this relation to obtain the standard
 991 quenched free energy expression [43, 44]

992
 993
$$\mathcal{F}_{\text{quenched}} = -k_B T \langle \langle \ln \mathcal{Z}_{\text{ci}} \rangle \rangle. \quad (81)$$

994
 995 All other values of n represent a partially annealed situation. The quenched limit translates
 996 into an infinite temperature for the disorder [43, 44, 55–64] relative to counterions, reflecting
 997 the fact that the statistics of quenched disorder is unaffected by counterions. It also reflects
 998 the zero mobility of surface charges when the dynamical interpretation *via* Einstein’s relation
 999 is used (assuming a finite surface diffusion coefficient).

Appendix C: Effective Surface Charge Density

The effective surface charge density σ_{eff} in the two-plate system is defined via

$$\sigma_{\text{eff}} = -\frac{1}{2Se_0} \int d\mathbf{r} [[\rho(\mathbf{r})]], \tag{82}$$

where $[[\dots]] = \frac{1}{\mathcal{Z}} \int \mathcal{D}\rho \mathcal{P}[\rho] (\mathcal{Z}_{\text{ci}}[\rho])^n (\dots)$ is the full ensemble average with respect to the partition function \mathcal{Z} , (4). It may be written in terms of $\langle\langle \dots \rangle\rangle$ averages defined after (4) as $[[\dots]] = \langle\langle (\mathcal{Z}_{\text{ci}}[\rho])^n (\dots) \rangle\rangle / \langle\langle (\mathcal{Z}_{\text{ci}}[\rho])^n \rangle\rangle$. One can easily show from (4) and (8) that

$$[[\rho(\mathbf{r})]] = \rho_0(\mathbf{r}) + g(\mathbf{r}) \frac{\delta \ln \mathcal{Z}}{\delta \rho_0(\mathbf{r})} = \rho_0(\mathbf{r}) - i\beta g(\mathbf{r}) \sum_a [[\phi_a(\mathbf{r})]]. \tag{83}$$

Obviously, the effective or renormalized surface charge is shifted from the bare value, $\rho_0(\mathbf{r})$, by an amount proportional to the mean surface potential $[[\phi_a(\mathbf{r})]]$. Thus the charge renormalization in the present context is rendered *via* a linear surface screening mechanism (as may be seen also from the quadratic disorder terms $g(\mathbf{r})\phi_a(\mathbf{r})\phi_b(\mathbf{r})$ in the effective Hamiltonian (9)). This can be traced back to the Gaussian approximation for the disorder distribution, (5).

It follows immediately from (83) that no charge renormalization occurs in the quenched limit ($n \rightarrow 0$) and it may be possible only for a partially annealed disorder ($n > 0$). Assuming the replica symmetry *ansatz*, one can recover the PB effective charge, (14) and (19), in the mean-field limit. In the SC limit, the effective charge and the fugacity, λ , are determined simultaneously from (82) and (83) above combined with (51) or (52) in the text and the electroneutrality condition $Nq = 2\sigma_{\text{eff}}S$, *i.e.*

$$\lambda = \frac{2\sigma_{\text{eff}}S}{q \int d\mathbf{R} \Omega(\mathbf{R}) e^{-\beta u(\mathbf{R})}}, \tag{84}$$

$$\sigma_{\text{eff}} = -\frac{1}{2Se_0} \int d\mathbf{r} \left[\rho_0(\mathbf{r}) + g(\mathbf{r}) \frac{\delta \ln \mathcal{Z}}{\delta \rho_0(\mathbf{r})} \right]. \tag{85}$$

By using the SC results for the single-particle interaction, u , and the partition function, \mathcal{Z} , from Sects. 4.2 and 4.3, and expanding σ_{eff} and λ in powers of n as

$$\sigma_{\text{eff}} = \sigma^{(0)} + n\sigma^{(1)} + \dots, \tag{86}$$

$$\lambda = \lambda^{(0)} + n\lambda^{(1)} + \dots, \tag{87}$$

we find that $\sigma^{(0)} = \sigma$, $\lambda^{(0)} = 2\sigma S/q \int d\mathbf{R} \Omega(\mathbf{R}) e^{-\beta u_0(\mathbf{R})}$, and

$$\frac{\sigma^{(1)}}{\sigma} = \frac{\beta}{2\sigma Se_0} \int d\mathbf{r} g(\mathbf{r}) \left[\langle \rho_0 | \hat{v}_s | \mathbf{r} \rangle + qe_0 \lambda^{(0)} \int d\mathbf{R} \Omega(\mathbf{R}) e^{-\beta u_0(\mathbf{R})} \langle \mathbf{r} | \hat{v}_s | \mathbf{R} \rangle \right], \tag{88}$$

$$\frac{\lambda^{(1)}}{\lambda^{(0)}} = \frac{\sigma^{(1)}}{\sigma} - \beta \frac{\int d\mathbf{R} \Omega(\mathbf{R}) u_1(\mathbf{R}) e^{-\beta u_0(\mathbf{R})}}{\int d\mathbf{R} \Omega(\mathbf{R}) e^{-\beta u_0(\mathbf{R})}}. \tag{89}$$

The $\lambda^{(1)}$ term and other higher-order terms lead to higher-order contributions in the effective charge and thus will not be relevant here. By straightforward calculations and using the results in the text, one can show that

$$\frac{\sigma^{(1)}}{\sigma} = g\ell_B \left(\frac{2\pi}{\kappa} \right) \left[- (1 + e^{-\kappa d}) + \frac{\int d\mathbf{R} \Omega(\mathbf{R}) e^{-\beta u_0(\mathbf{R})} (e^{-\kappa|a-R_z|} + e^{-\kappa|a+R_z|})}{\int d\mathbf{R} \Omega(\mathbf{R}) e^{-\beta u_0(\mathbf{R})}} \right]. \tag{90}$$

1051 In the limit $\kappa \rightarrow 0$, the first two terms in the bracket on the right hand side are cancelled by
 1052 similar contributions from the integrals in the last term and one can show that

1053

1054

1055

$$\lim_{\kappa \rightarrow 0} \frac{\sigma^{(1)}}{\sigma} = 0. \quad (91)$$

1056

1057

1058

1059

1060

1061

1062

References

1063

1064

1065

1066

1067

1068

1069

1070

1071

1072

1073

1074

1075

1076

1077

1078

1079

1080

1081

1082

1083

1084

1085

1086

1087

1088

1089

1090

1091

1092

1093

1094

1095

1096

1097

1098

1099

1100

1. Schena, M., Shalon, D., Davis, R.W., Brown, P.O.: *Science* **270**, 467 (1995)
2. Halperin, A., Buhot, A., Zhulina, E.B.: *Biophys. J.* **86**, 718 (2004)
3. Meyer, E.E., Lin, Q., Hassenkam, T., Oroudjev, E., Israelachvili, J.N.: *Proc. Natl. Acad. Sci. USA* **102**, 6839 (2005)
4. Perkin, S., Kampf, N., Klein, J.: *Phys. Rev. Lett.* **96**, 038301 (2006)
5. Perkin, S., Kampf, N., Klein, J.: *J. Phys. Chem. B* **109**, 3832 (2005)
6. Meyer, E.E., Rosenberg, K.J., Israelachvili, J.: *Proc. Natl. Acad. Sci. USA* **103**, 15739 (2006)
7. Kantor, Y., Li, H., Kardar, M.: *Phys. Rev. Lett.* **69**, 61 (1992)
8. Borukhov, I., Andelman, D., Orland, H.: *Eur. Phys. J. B* **5**, 869 (1998)
9. Lipowsky, R., Sackmann, E. (eds.): *Handbook of Biological Physics: Structure and Dynamics of Membranes*. Elsevier, Amsterdam (1995)
10. Ninham, B.W., Parsegian, V.A.: *J. Theor. Biol.* **31**, 405 (1971)
11. Chan, D., Perram, J.W., White, L.R., Healy, T.W.: *J. Chem. Soc. Faraday Trans. I* **71**, 1046 (1975)
12. Chan, D., Healy, T.W., White, L.R.: *J. Chem. Soc. Faraday Trans. I* **72**, 2844 (1976)
13. Verwey, E.J.W., Overbeek, J.Th.G.: *Theory of the Stability of Lyophobic Colloids*. Elsevier, Amsterdam (1948)
14. Israelachvili, J.N.: *Intermolecular and Surface Forces*. Academic Press, London (1990)
15. Parsegian, V.A.: *Van der Waals Forces*. Cambridge University Press, Cambridge (2005)
16. Andelman, D.: In: Lipowsky, R., Sackmann, E. (eds.) *Handbook of Biological Physics: Structure and Dynamics of Membranes*, vol. 1B. Elsevier, Amsterdam (1995). Chap. 12
17. Podgornik, R., Žekš, B.: *J. Chem. Soc. Faraday Trans. II* **84**, 611 (1988)
18. Podgornik, R.: *J. Chem. Phys.* **91**, 5840 (1989)
19. Podgornik, R.: *J. Phys. A: Math. Gen.* **23**, 275 (1990)
20. Boroudjerdi, H., Kim, Y.W., Naji, A., Netz, R.R., Schlagberger, X., Serr, A.: *Phys. Rep.* **416**, 129 (2005)
21. Naji, A., Jungblut, S., Moreira, A.G., Netz, R.R.: *Physica A* **352**, 131 (2005)
22. Netz, R.R.: *Eur. Phys. J. E* **5**, 557 (2001)
23. Grosberg, A.Yu., Nguyen, T.T., Shklovskii, B.I.: *Rev. Mod. Phys.* **74**, 329 (2002)
24. Levin, Y.: *Rep. Prog. Phys.* **65**, 1577 (2002)
25. Moreira, A.G., Netz, R.R.: *Europhys. Lett.* **57**, 911 (2002)
26. Lukatsky, D.B., Safran, S.A.: *Europhys. Lett.* **60**, 629 (2002)
27. Kanduč, M., Trulsson, M., Naji, A., Burak, Y., Forsman, J., Podgornik, R.: *Phys. Rev. E* (2008, in press)
28. Naji, A., Podgornik, R.: *Phys. Rev. E* **72**, 041402 (2005)
29. Podgornik, R., Naji, A.: *Europhys. Lett.* **74**, 712 (2006)
30. Fleck, C., Netz, R.R.: *Europhys. Lett.* **70**, 341 (2005)
31. Fleck, C., Netz, R.R.: *Eur. J. Phys. E* **22**, 261 (2007)
32. Fleck, C., Netz, R.R., von Grünberg, H.H.: *Biophys. J.* **82**, 76 (2002)
33. Nguyen, T.T., Grosberg, A.Yu., Shklovskii, B.I.: *J. Chem. Phys.* **113**, 1110 (2000)
34. Foret, L., Kühn, R., Würger, A.: *Phys. Rev. Lett.* **89**, 156102 (2002)
35. Russ, C., Heimbürg, T., von Grünberg, H.H.: *Biophys. J.* **84**, 3730 (2003)
36. Harries, D., Podgornik, R., Parsegian, V.A., Mar-Or, E., Andelman, D.: *J. Chem. Phys.* **124**, 224702 (2006)
37. Gelbart, W.M., Bruinsma, R.: *Phys. Rev. E* **55**, 831 (1997)
38. Kim, Y.W., Sung, W.: *Phys. Rev. Lett.* **91**, 118101 (2003)
39. Hed, G., Safran, S.A.: *Phys. Rev. Lett.* **93**, 138101 (2004)
40. Kanduč, M., Podgornik, R.: *Eur. Phys. J. E* **23**, 265 (2007)

Partially Annealed Disorder and Collapse of Like-Charged Macroions

1101 41. Jho, Y.S., Kanduć, M., Naji, A., Podgornik, R., Kim, M.W., Pincus, P.A.: Phys. Rev. Lett. (2008, in
 1102 press)
 1103 42. Punkkinen, O., Naji, A., Podgornik, R., Vattulainen, I., Hansen, P.-L.: Europhys. Lett. **82**, 48001 (2008)
 1104 43. Dotsenko, V.: Introduction to the Replica Theory of Disordered Statistical Systems. Cambridge Univer-
 1105 sity Press, New York (2001)
 1106 44. Dotsenko, V.: An Introduction to the Theory of Spin Glasses and Neural Networks. World Scientific,
 1107 Singapore (1994)
 1108 45. Manne, S., Cleveland, J.P., Gaub, H.E., Stucky, G.D., Hansma, P.K.: Langmuir **10**, 4409 (1994)
 1109 46. Manne, S., Gaub, H.E.: Science **270**, 1480 (1995)
 1110 47. Zhang, G., Marie, P., Maaloum, M., Muller, P., Benoit, N., Krafft, M.P.: J. Am. Chem. Soc. **127**, 10412
 1111 (2005)
 1112 48. Haken, H.: Synergetics, an Introduction. Springer, Berlin (1983)
 1113 49. Risken, H.: The Fokker-Planck Equation. Springer, Berlin (1989)
 1114 50. Kaneko, K.: Prog. Theor. Phys. **66**, 129 (1981)
 1115 51. Landauer, R., Woo, J.W.F.: Phys. Rev. A **6**, 2204 (1972)
 1116 52. Allahverdyan, A.E., Petrosyan, K.G.: Phys. Rev. Lett. **96**, 065701 (2006)
 1117 53. Allahverdyan, A.E., Nieuwenhuizen, Th.M.: Phys. Rev. Lett. **85**, 232 (2000)
 1118 54. Allahverdyan, A.E., Nieuwenhuizen, Th.M.: Phys. Rev. E **62**, 845 (2000)
 1119 55. Coolen, A.C.C., Penney, R.W., Sherrington, D.: Phys. Rev. B **48**, 16116 (1993)
 1120 56. Penney, R.W., Coolen, A.C.C., Sherrington, D.: J. Phys. A: Math. Gen. **26**, 3681 (1993)
 1121 57. Dotsenko, V., Franz, S., Mézard, M.: J. Phys. A: Math. Gen. **27**, 2351 (1994)
 1122 58. Penney, R., Sherrington, D.: J. Phys. A: Math. Gen. **27**, 4027 (1994)
 1123 59. Caticha, N.: J. Phys. A: Math. Gen. **27**, 5501 (1994)
 1124 60. Feldman, D.E., Dotsenko, V.S.: J. Phys. A: Math. Gen. **27**, 4401 (1994)
 1125 61. Jogen, G., Bolle, D., Coolen, A.C.C.: J. Phys. A: Math. Gen. **31**, L737 (1998)
 1126 62. Jongen, G., Anemüller, J., Bolle, D., Coolen, A.C.C., Perez-Vicente, C.: J. Phys. A: Math. Gen. **34**, 3957
 1127 (2001)
 1128 63. Kondor, I.: J. Phys. A: Math. Gen. **16**, L127 (1983)
 1129 64. Allahverdyan, A.E., Nieuwenhuizen, Th.M., Saakian, D.B.: Eur. Phys. J. B **16**, 317 (2000)
 1130 65. Dean, D.S.: J. Phys. A: Math. Gen. **29**, L613 (1996)
 1131 66. Archer, A.J., Rauscher, M.: J. Phys. A: Math. Gen. **37**, 9325 (2004)
 1132 67. Marconi, U.M.B., Tarazona, P.: J. Chem. Phys. **110**, 8032 (1999)
 1133 68. Hohenberg, P.C., Halperin, B.I.: Rev. Mod. Phys. **49**, 435 (1977)
 1134 69. Ma, S.-K.: Modern Theory of Critical Phenomena. Benjamin, Massachusetts (1976)
 1135
 1136
 1137
 1138
 1139
 1140
 1141
 1142
 1143
 1144
 1145
 1146
 1147
 1148
 1149
 1150